2017 American Control Conference
Sheraton Seattle Hotel
May 24–26, 2017, Seattle, USA

A Synthetic Input Approach to Slip Angle Based Steering Control for Autonomous Vehicles

John K. Subosits[1,2] and J. Christian Gerdes[1]

Abstract— **A new method is presented for low-level steering control of autonomous vehicles. By tracking tire slip angle instead of steering angle, the new controller makes possible a more direct use of force-based high-level control schemes since uncertain, noisy measurements of the vehicle states do not have to be used to convert a desired tire slip angle to a commanded steer angle. Experimental data from a full-size vehicle show that this approach offers some advantages when combined with a force-based path tracking controller. Improved steering control and path tracking performance are demonstrated, particularly at the limits of tire friction, and the reasons for these improvements are briefly discussed.**

I. INTRODUCTION

The introduction of autonomous vehicles promises to both improve road safety and reduce wasted travel time. The problem of designing high-level steering controllers for autonomous vehicles has led to the publication of a number of approaches. However, all approaches must address two fundamental challenges. The first is that the relationship between the lateral force generated by a tire and its slip angle is nonlinear because of the limited friction between the tire and the road. To cover all driving situations, a controller must be robust to the fact that a saturated tire can produce no more force. The second challenge is the need to balance control design difficulty and required computation time with the task scope and the required performance. As the state of the art in control of autonomous vehicles evolves from simply path tracking to navigating in dynamic, real world environments, there is a need for low-level control approaches that lessen the burden on high-level planning and control modules.

Schemes for determining a steering angle to track a path, even up to the friction limits of the tires, using both Model Predictive Control [1] and more conventional state feedback design [2] are available in the literature. Tracking the desired steering angle with the steering actuator is a servomechanism problem which is solved with a PID controller or a lead compensator [3], [4]. Recent work has demonstrated that steering torque can be used as the control input for path tracking directly, at least for relatively sedate maneuvers [5]. While steering angle may seem to be the obvious choice as a control input, using front lateral tire force makes the system dynamics linear in the control input. This approach, used for autonomous path tracking with MPC by Brown et al., also makes handling the friction limits of the tires straightforward [6]. However, while force is used as the control variable in the optimization routine, this is still effectively a steer angle based controller since an optimal lateral force is converted to a slip angle using a tire model and then to a steer angle using accurate, smooth measurements of the vehicle state.

Initially motivated by a need to reduce the dependence of the commanded steer angle on measurements when using a force-based controller, we present a low-level steering controller designed to track a desired slip angle for the front tires. This slip angle is provided by a higher level controller, either directly or by conversion of a desired lateral force via an inverse tire model. Experimental data collected from a fully autonomous testbed demonstrate that the new controller is capable of outperforming an existing steer angle based control scheme in angular tracking which leads to improved path tracking by the vehicle. This approach can be pushed all the way to the limits of both the vehicle and the steering actuator.

The following sections introduce the design of the slip angle controller and demonstrate its effectiveness through a series of tests on a full-scale autonomous vehicle. First, the necessary dynamics of an automobile and its steering system and the controller derivation are presented. Next, data showing the improved performance of a force-based controller similar to the one in [6] are presented and briefly analyzed. To demonstrate the performance of the slip angle based control scheme at maximum friction usage and to provide a more direct comparison, results with an angle-based controller handling the path tracking are given. In these tests, better tracking of the desired slip or steer angle leads to improved path tracking accuracy.

II. CONTROLLER DESIGN

In this section, we introduce a controller that uses the torque produced by a power steering motor to cause the front tires of an autonomous vehicle to track a desired slip angle. The design leverages knowledge of the dynamics of both the vehicle and the steering system. The controller is of a nested loop design with a desired steering wheel velocity used as a synthetic input to the inner loop. Feedback linearization is used in each loop to allow the desired, exponentially stable dynamics to be imposed. The overall control structure is illustrated in Fig. 1.

A. Model of Vehicle and Steering System

While steer angle can be measured directly, computing slip angle requires information about the vehicle state. The state variables of the planar single track model used in this work are defined in Fig. 2. For slip angle tracking, the position and orientation of the vehicle are not relevant, but the longitudinal

[1]Department of Mechanical Engineering, Stanford University, Stanford, CA 94305, USA
[2]Corresponding author, subosits@stanford.edu

velocity u_x, the lateral velocity u_y, and the yaw rate r are all used. The front slip angle, α_f, can be computed from available measurements of the vehicle state and the steer angle δ as

$$\tan\alpha_f = \frac{(u_y + ar)\cos\delta - u_x \sin\delta}{u_x \cos\delta + (u_y + ar)\sin\delta} \tag{1}$$

where a is the distance from the center of mass to the center of the front axle. For the purpose of control design, this expression can be simplified to

$$\alpha_f \approx \frac{u_y + ar}{u_x} - \delta. \tag{2}$$

by assuming the steer and slip angles are small in magnitude.

The tire forces dominate the motion of the vehicle. Neglecting contributions from longitudinal forces at the front wheels gives the following equations for the lateral dynamics of the vehicle:

$$\dot{r} = \frac{aF_{yf}\cos\delta - bF_{yr}}{I_{zz}} \tag{3}$$

and

$$\dot{u_y} = \frac{F_{yr} + F_{yf}\cos\delta}{m} - ru_x \tag{4}$$

where m is the vehicle mass and I_{zz} is the moment of inertia about the center of mass.

Many tire models, both theoretical and empirical, that relate the slip angle of the tires to the lateral force are available. In this work, a single friction coefficient Fiala model was found to be sufficient, but any model can be used to supply the the level of accuracy desired. The tire lateral force is given by

$$F_y = -C_\alpha \tan\alpha + \frac{C_\alpha^2}{3\mu F_z}|\tan\alpha|\tan\alpha - \frac{C_\alpha^3}{27(\mu F_z)^2}\tan^3\alpha \tag{5}$$

when $|\tan\alpha| < \frac{3\mu F_z}{C_\alpha}$. If the slip angle exceeds this threshold, the tire is said to be fully saturated and $F_y = -\mu F_z \mathrm{sgn}\tan\alpha$. Operating the tire in this regime is undesirable because the entire contact patch is sliding across the road, and, at least in this model, changing the slip angle has no effect on the lateral force. An important advantage of this model is that the friction coefficient μ and the cornering stiffness C_α are the only two parameters that must be identified.

A model of the dynamics of the steering system including external disturbance torques is also needed. The dynamics of the steering system are modeled as

$$\ddot{\delta} = \frac{\tau + f(F_{yf}, \delta)}{I} \tag{6}$$

where τ is the torque applied by the motor and I is the lumped inertia of the steering system referenced to the angular acceleration of the roadwheels. The two most significant external torques on the steering system are the moment from the lateral force generated by the front tires and the so-called jacking torque. An expression for these two forces is given by

$$f(F_{yf}, \delta) = -F_{yf}d_x - d_y F_{zf}\sin\lambda\sin\delta \tag{7}$$

where d_y and d_x are the lateral and longitudinal distances, respectively, between the center of the tire contact patch and the intersection of the steering axis with the ground and F_{zf} is the normal force on the front tires from the ground [7]. The lateral inclination angle of the steering axis is denoted by λ. Other effects that are not modeled in this work are torques arising from the pneumatic trail of the tire and differences in normal and longitudinal force on the front tires.

B. Derivation

Choosing the simplest possible form of exponentially stable dynamics for the difference between the actual and desired slip angle, we have

$$\dot{\alpha}_f - \dot{\alpha}_{f,des} = -K_1(\alpha_f - \alpha_{f,des}). \tag{8}$$

Differentiating (2) with respect to time gives:

$$\dot{\alpha}_f = \frac{\dot{u}_y + a\dot{r}}{u_x} - \frac{\dot{u}_x(u_y + ar)}{u_x^2} - \dot{\delta}. \tag{9}$$

The second term is neglected in this work because u_x is much larger than $\dot{u}_x$ for a vehicle moving under control at an appreciable speed. Using (8) and (9) to eliminate $\dot{\alpha}_f$ gives

$$\dot{\delta}_{des} = K_1(\alpha_f - \alpha_{f,des}) - \dot{\alpha}_{f,des} + \frac{\dot{u}_y + a\dot{r}}{u_x} \tag{10}$$

where $\dot{\delta}_{des}$ is the synthetic input to the inner loop in the nested loop structure.

Likewise for the steering system, we have the desired error dynamics

$$\ddot{\delta} - \ddot{\delta}_{des} = -K_2(\dot{\delta} - \dot{\delta}_{des}). \tag{11}$$

As is typical with nested loop control designs, K_2 is chosen to be 5 to 10 times larger than K_1 so that the inner loop is driven to steady-state quickly enough to avoid any significant coupling with the error dynamics of the outer loop. From (6) and (11), the torque requested of the steering motor is found to be

$$\tau = I(-K_2(\dot{\delta} - \dot{\delta}_{des})) - f(F_{yf}, \delta) \tag{12}$$

where we have elected to treat $\ddot{\delta}_{des}$ as a disturbance. Alternatives to this approach are considered in section II-C. Substituting the expression for $\dot{\delta}_{des}$ from (10) yields a final expression for the control torque:

C. Practicalities of Implementation

Not all the terms appearing in the control law are available directly from measurements. The derivative of the reference slip angle can be found from the predicted future control inputs in an MPC framework, numerical differentiation, or analytical computation in some cases. All approaches were found to work in testing. Similarly, a measurement of $\dot{\delta}$ is not available on the test vehicle; only δ is measured. Direct numerical differentiation is used to estimate $\dot{\delta}$. Likewise, measurements of $\dot{r}$ are not available directly. Differentiating the noisy yaw rate signal was deemed impractical, and values of $\dot{u}_y$ computed using lateral acceleration measurements, $\dot{u}_y = a_y - ru_x$, are noisy. Instead, the tire and vehicle models were used to predict these terms. Measurements and

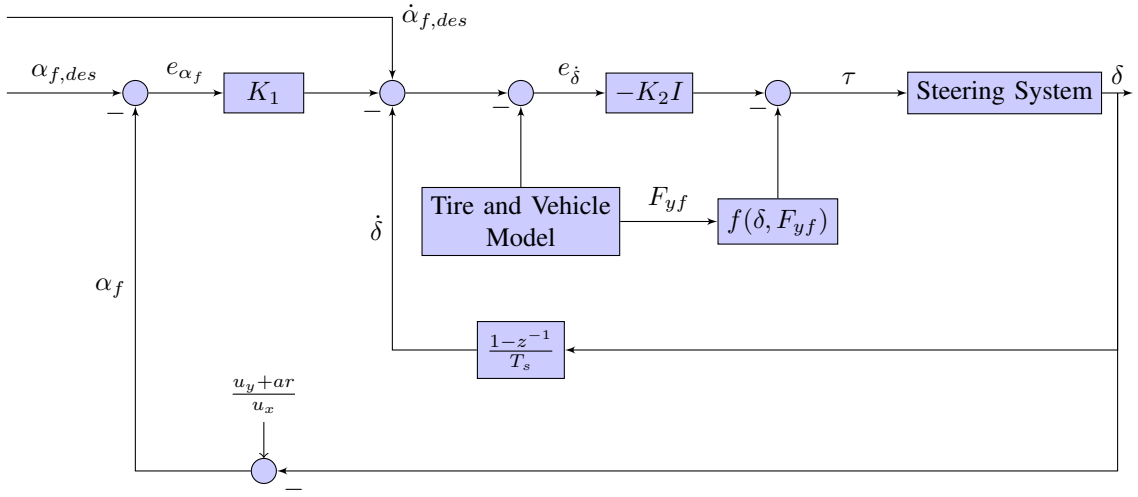

Fig. 1. A diagram of the proposed control scheme.

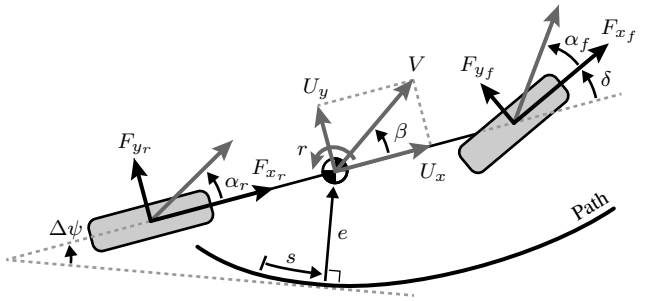

Fig. 2. Schematic of the single-track model with vehicle states and path tracking states

models could be combined using state estimation techniques if modeling error is a concern, but the simple models used here gave acceptable performance.

Finding $\ddot{\delta}_{des}$ analytically to a useful accuracy is difficult since it requires differentiating an uncertain vehicle model. A predictive controller that generates an expected series of commands and vehicle states could provide this signal. Another option is a Dynamic Surface Controller [8], which uses an approximation achieved by numerically differentiating a filtered version of $\dot{\delta}_{des}$. This method actually provides guaranteed performance for an appropriate choice of the filter constant. Practically, this term can be treated as a disturbance and left to the feedback law to handle.

The problem of defining the slip angle at low speeds must also be overcome. The longitudinal velocity, u_x appears in the denominator of the expressions for the slip angle and the desired steer angle rate. Division by zero is avoided by bounding the magnitude of u_x from below by a small positive constant. However, at low speeds the controller is still sensitive to measurement inaccuracy, but this problem is handled by modeling the tire relaxation length. The tire relaxation length, l_r, accounts for the fact that a tire brought to a new slip angle instantaneously will not deform and generate force immediately. A model for this process is

$$\dot{\bar{\alpha}} = -\frac{u_x}{l_r}(\bar{\alpha} - \alpha) \tag{13}$$

where $\bar{\alpha}$ models the deflection of the section of tire in contact with the ground and l_r is typically a fraction of the radius of the tire. The corrected slip angle, $\bar{\alpha}$, matches α to within measurement accuracy while driving, and can be used as the input to the vehicle model and as the measurement for the steering controller.

III. Experimental Results

This controller design was tested on a fully autonomous 2009 Audi TTS with command of steering torque, brake pressure, and gear selection via multiple Controller Area Network buses and of throttle through a direct analog signal. The vehicle is instrumented with an Oxford Technical Solutions RT4003 dual-antenna GPS/INS unit for accurate measurement of vehicle states. Actuation is provided by a standard electric assist power steering rack which accepts torque commands at 100 Hz from the steering controller running on a dSPACE MicroAutoBox. Measurement of the steer angle at the rack is in terms of steering column, not roadwheel rotation, so a nonlinear mapping is used to convert it. The steering column introduces an unmodeled, lightly damped structural mode with a resonant frequency of approximately 11 Hz. For this vehicle, an outer loop gain of $K_1 = 19$ and an inner loop gain of $K_2 I = 10$ was found to work well. Note that the time constant of the inner loop is much faster than that of the outer loop because the system inertia is approximately 0.1 kg m^2 although this value is difficult to determine precisely. All data presented in this paper are collected from the autonomous operation of this vehicle over Turns 2-4 at Thunderhill Raceway in Willows, CA.

For evaluation, the slip angle tracking controller is compared to an existing steer angle based controller. The older controller uses a feedforward torque with feedback torque

Fig. 3. Fully autonomous Audi TTS

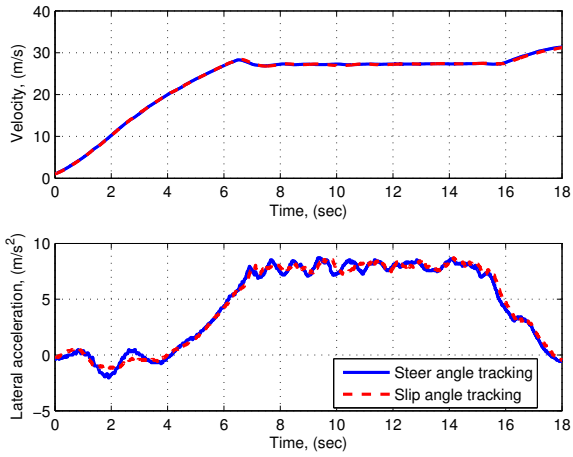

Fig. 4. An illustration of the driven trajectory.

determined by a lead compensator that acts on the error in steer angle. When considering radians of error at the roadwheels, the transfer function of the compensator is

$$K(s) = \frac{149.8(0.05s+1)}{0.014s+1} = 149.8 + \frac{5.39s}{0.014s+1}. \quad (14)$$

The compensator is implemented at a sampling rate of 10 ms using forward Euler discretization. The feedforward torque is computed using the same model of the torques acting on the steering system as in the slip angle tracking controller, i.e. $f(F_{yf}, \delta)$. However, since it is being used for feedforward control instead of feedback linearization, feedforward values for F_{yf} and δ are used instead of measurements.

A. Force-based Path Tracking Controller

Tests conducted over identical reference trajectories using the force-based path tracking controller in [6] show two reasons to consider using slip angle instead of steer angle in low-level control. The measured speed and lateral acceleration are shown in Fig 4. The desired trajectory is fairly aggressive, with required lateral accelerations of 7.5 m/s^2, but is still well within the friction limits of the tires.

The performance of the steer angle tracking controller is shown in Fig. 5, and the slip angle controller performance is shown in Fig. 6. During "normal" operation of the controller, when the vehicle speed is greater than 10 m/s, starting at about 2 seconds in the plots, the slip angle controller tracks the reference signal more closely. The slip angle reference

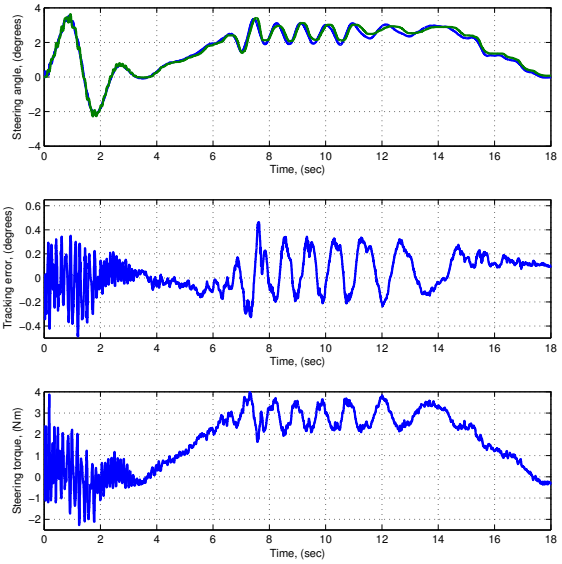

Fig. 5. Tracking performance of the steer angle tracking controller

signal has less variation, and is easier to track, partly because the optimization based path tracking controller penalizes changes in lateral force and therefore slip angle directly. Path tracking performance is actually quite similar between the two controllers, but the slip angle controller results in less oscillatory behavior for the yaw rate of the vehicle as shown in Fig. 7. The tighter tracking and faster response to transients of the slip angle controller leads to better yaw damping and therefore smaller variations in the force and slip angle commanded by the path tracking controller.

In addition to smaller oscillations about the steady-state yaw rate in the corner, the slip angle controller also displays more desirable behavior at low speed. Here, the conversion from desired slip angle to desired steer angle introduces high frequency, if low amplitude, oscillation in the steering command that are difficult for the controller to track. Meanwhile, the slip angle controller is able to work with an estimate of the slip angle which is made smooth through the relaxation length. This filtering means that the slip angle controller produces a much smoother response at low speed resulting in less oscillation in both yaw rate and lateral error as the vehicle drives itself onto the path at the start of the test.

B. Angle Based Path Tracking Controller

Unfortunately, the force-based path following controller does not yet perform well on this vehicle at high speeds and the limits of tire friction. To assess the behavior of the slip angle based steering controller under these conditions, a path tracking controller [2] that is known to work well at the friction limits is modified to command a slip angle instead of a steering angle as described in the appendix. Three trials were conducted with each steering controller over the trajectory shown in Fig. 8 which requires full use

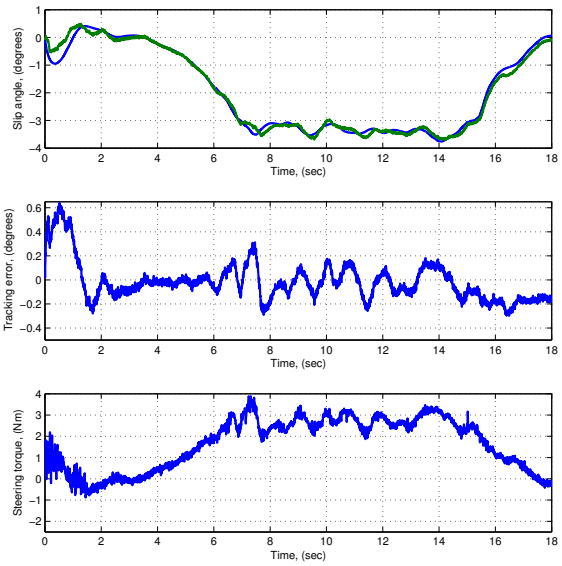

Fig. 6. Tracking performance of the slip angle tracking controller

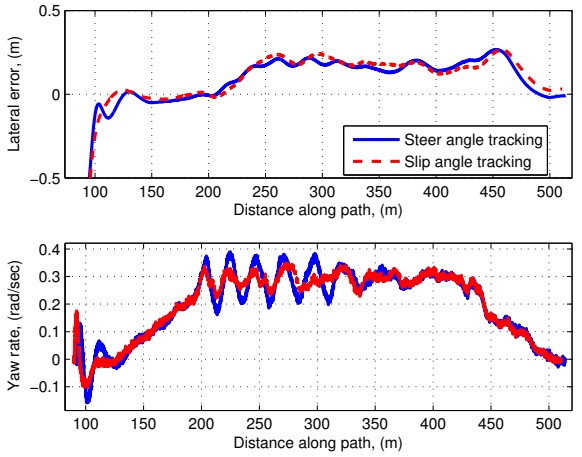

Fig. 7. Comparison of path tracking performance of the two controllers

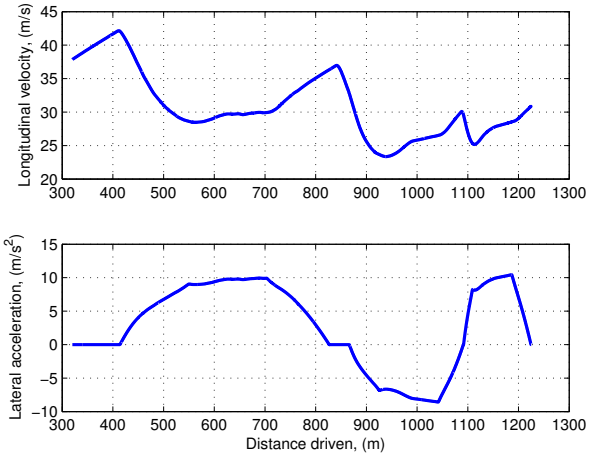

Fig. 8. An illustration of the desired trajectory.

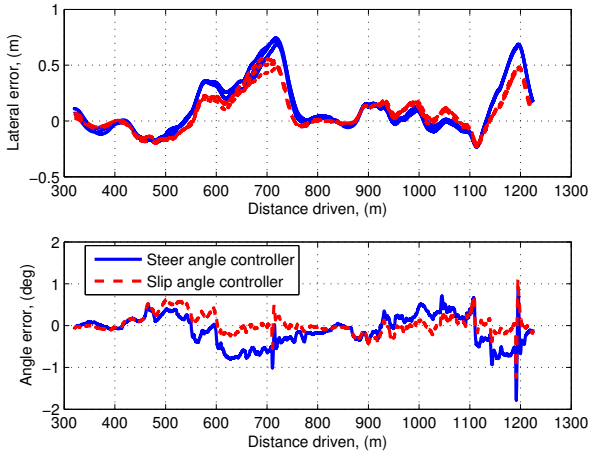

Fig. 9. Relationship between path tracking and average angle tracking performance

of the friction of the tires. In places, the required lateral acceleration can exceed 1 g because of the banking of the track.

The slip angle tracking steering controller was found to consistently produce smaller tracking errors than the steer angle tracking controller as is shown in Figure 9. The rms value of the tracking error for the slip angle controller is 0.22 degrees which is substantially less than the value of 0.35 degrees for the steer angle tracking controller. The rms value of the lateral error of the vehicle from the path shows a corresponding decrease from 0.25 meters to 0.19 meters. The average maximum lateral error across the 3 trials is 0.72 meters with the steer angle controller, but only 0.52 meters with the slip angle controller. The locations of reduced path tracking error correlate strongly with improved precision from the slip angle tracking controller.

IV. Analysis

The improved performance of the slip angle tracking controller over the baseline compensator is partly due to higher feedback gains. The proportional feedback gain from radians of position error to Newton-meters of motor torque is 27% higher at 190 versus 149.8. Clearly, this increased DC gain is a factor in the reduction of steady state offset. However, increased damping mitigates the reduction in stability margins. Furthermore, no phase lag is introduced through a low-pass filter, allowing tighter tracking of the higher frequency portions of the reference signal. The problem of noise attenuation is dealt with through incorporation of a vehicle model which eliminates numerical differentiation of the noisiest measurements.

While the torque command from the new controller contains more high frequency content, no adverse effects such as chatter from backlash in the steering gearbox or motor

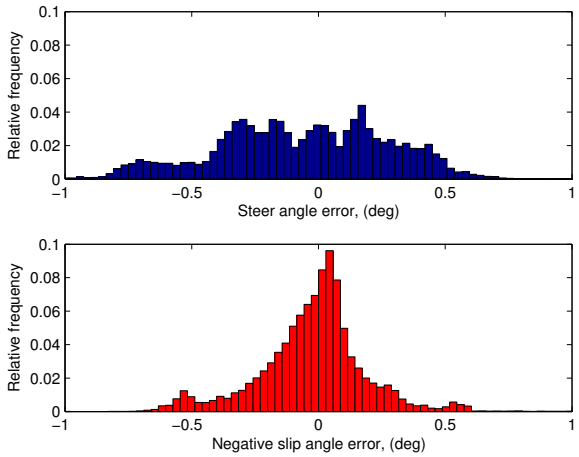

Fig. 10. Distribution of tracking error for both controllers

hum were observed. Excitation of the resonant mode of the steering column was also avoided. It is possible that the additional high frequency content acts as a dither signal and helps overcome small unmodeled effects such as stiction in the steering system. The observation from Fig. 10 that the distribution of tracking error with the old controller lacks a distinct peak at zero partially supports this conclusion.

V. CONCLUSIONS

In this paper, a slip angle tracking steering controller design is presented. Experimental data show that this controller compliments a lateral force-based path tracking controller. A direct comparison shows that the improved steer angle tracking achieved with this controller leads to better path tracking at the limits of friction. These data provide some insight into the relationship between high-level and low-level steering performance for autonomous vehicles.

Some possible extensions to this work include determination of a model that more accurately approximates the moments from the tires acting on the steering system. An additional improvement would be the incorporation of a $\ddot{\delta}_{des}$ signal, likely through a Dynamic Surface Controller.

APPENDIX

Here, we show how the steer angle based controller in [2] can be converted to an equivalent slip angle based controller. For a vehicle of wheelbase L traveling on a path with instantaneous curvature k, the existing controller has $\delta = \delta_{FFW} + \delta_{FBK}$ where

$$\delta_{FFW} = (kL + \alpha_{R,FFW} - \alpha_{F,FFW}) \tag{15}$$

and

$$\delta_{FBK} = (-K_p(e + x_{LA}(\Delta\psi + \beta_{FFW}))) \tag{16}$$

with $\beta_{FFW} = \alpha_{R,FFW} + bk$.

The goal when deriving the controller with slip angle as the command is to choose a slip angle so that the error in slip angle is equal in magnitude but opposite in sign to the error in steer angle obtained with the original path tracking controller. Note that this requires u_y and r be used to determine a slip angle angle although they are not used for steer angle. Accordingly, we set $\alpha = \alpha_{FFW} + \alpha_{FBK}$ where α_{FFW} is chosen by the same method as above. The feedback component of the slip angle is determined by

$$\alpha_{FBK} = -\delta_{FBK} + \arctan\frac{u_y + ar}{u_x} - \arctan\frac{(u_y + ar)_{FFW}}{u_x}. \tag{17}$$

To determine the desired rate of change for the slip angle, direct measurements are used where possible. Differentiating the expression for δ_{FBK} gives

$$\dot{\delta}_{FBK} = (-K_p(\dot{e} + x_{LA}(\dot{\Delta\psi} + \dot{\beta_{FFW}}))) \tag{18}$$

where

$$\dot{e} = (u_x \sin\Delta\psi + u_y \cos\Delta\psi) \tag{19}$$

and

$$\dot{\Delta\psi} = r - \frac{k}{1 - ke}(u_x \cos\Delta\psi - u_y \sin\Delta\psi) \tag{20}$$

can be computed from measurements. Changes in the feedforward steering command are determined by finite differences. In conclusion, a path tracking controller designed to produce a steer angle command has been converted to use slip angle as a control signal.

ACKNOWLEDGMENT

J.K.S. thanks Samuel Schacher of Volkswagen Group Research for his assistance with initial tuning of the controller. Robin Simpson and Larry Dirksen of the Volkswagen Electronics Research Laboratory were instrumental in the preparation and maintenance of the testbed.

REFERENCES

[1] P. Falcone, F. Borrelli, J. Asgari, H. E. Tseng, and D. Hrovat, "Predictive active steering control for autonomous vehicle systems," *IEEE Transactions on Control Systems Technology*, vol. 15, no. 3, pp. 566–580, 2007.

[2] N. R. Kapania and J. C. Gerdes, "Design of a feedback-feedforward steering controller for accurate path tracking and stability at the limits of handling," *Vehicle System Dynamics*, vol. 53, no. 12, pp. 1687–1704, 2015.

[3] M. Wise and J. Hsu, "Application and analysis of a robust trajectory tracking controller for under-characterized autonomous vehicles," *2008 IEEE International Conference on Control Applications*, no. 1, pp. 274–280, 2008. [Online]. Available: http://ieeexplore.ieee.org/lpdocs/epic03/wrapper.htm?arnumber=4629651

[4] K. M. Kritayakirana, "Autonomous vehicle control at the limits of handling," Ph.D. dissertation, Stanford University, June 2012.

[5] E. Galceran, R. M. Eustice, and E. Olson, "Toward integrated motion planning and control using potential fields and torque-based steering actuation for autonomous driving," in *2015 IEEE Intelligent Vehicles Symposium (IV)*. IEEE, 2015, pp. 304–309.

[6] M. Brown, J. Funke, S. Erlien, and J. C. Gerdes, "Safe driving envelopes for path tracking in autonomous vehicles," *Control Engineering Practice*, 2016.

[7] T. D. Gillespie, *Fundamentals of Vehicle Dynamics*. Warrendale, PA: SAE, Inc., 1992.

[8] D. Swaroop, J. K. Hedrick, P. P. Yip, and J. C. Gerdes, "Dynamic surface control for a class of nonlinear systems," *IEEE Transactions on Automatic Control*, vol. 45, no. 10, pp. 1893–1899, 2000.